Published in final edited form as:
Magn Reson Med. 2012 October ; 68(4): 1273–1278. doi:10.1002/mrm.24112.

Pharmacological MRI of the choroid and retina: blood flow and BOLD responses during nitroprusside infusion

Yen-Yu I. Shih[1], **Guang Li**[1], **Eric R Muir**[1], **Bryan H De La Garza**[1], **Jeffrey W Kiel**[2], and **Timothy Q. Duong**[1,2,3,4,5]

[1]Research Imaging Institute, University of Texas Health Science Center

[2]Department of Ophthalmology, University of Texas Health Science Center

[3]Department of Radiology, University of Texas Health Science Center

[4]Department of Physiology, University of Texas Health Science Center

[5]South Texas Veterans Health Care System

Abstract

Nitroprusside, a vasodilatorynitric oxide donor, is clinically used during vascular surgery and to lower blood pressure in acute hypertension. This paper reports a novel application of blood flow (BF) and blood-oxygenation-level-dependent (BOLD) MRI on a 11.7 Tesla scanner to image the rat chorioretinal BF and BOLD changes associated with graded nitroprusside infusion. At low doses (1 or 2 μg/kg/min), nitroprusside increased BF as expected but decreased BOLD signals, showing an intriguing BF-BOLD uncoupling. At high doses (3–5 μg/kg/min) nitroprusside decreased BF and markedly decreased BOLD signals. To our knowledge, this is the first pharmacological MRI application of the retina. This approach has potential to open up new avenues to study the drug-related hemodynamic functions and evaluate the effects of novel therapeutic interventions on BOLD and BF in the normal and diseased retinas.

Keywords

Pharmacological MRI; retina; blood flow; BOLD; PO_2; nitroprusside; nitric oxide

Introduction

Nitroprusside, a nitric oxide (NO) (1) donor, is widely used to lower acute hypertension, treat acute decompensated heart failure (2,3), and control blood pressure during vascular surgery (4). Systemic infusion of nitroprusside decreases blood pressure and increases heart rate in humans and animals (5). Previous studies with NO donors and nitric oxide synthase inhibitors indicate that NO also plays an important role in ocular blood flow (BF) regulation (6-8). Other studies have shown that nitroprusside infusion increased retinal arteriolar and venular diameter (9,10) as well as choroidal BF (11) in animals. It also increased both venous and arterial retinal diameter and retinal leukocyte flow in healthy humans (12). NO dysfunction has been implicated in glaucoma, diabetic retinopathy, and retinal ischemia (6,13). Administration of nitroprusside can reverse the secondary arteriolar vasoconstriction observed after retinal branch vein occlusion so as to protect the retina against ischemic

Correspondence: Timothy Q Duong, Ph.D. (duongt@uthscsa.edu), or Yen-Yu Ian Shih, Ph.D. (shihy@uthscsa.edu), Research Imaging Institute, University of Texas Health Science Center at San Antonio, 8403 Floyd Curl Dr, San Antonio, TX 78229, Tel: 210-567-8120, Fax: 210-567-8152.
YYIS and GL contributed to this study equally

injury (14). Despite the widespread clinical use of nitroprusside, its effects on tissue perfusion and oxygenation in the retina remains poorly understood.

Recently, MRI has been used to image quantitative BF and relative tissue oxygenation in the retina. Blood-oxygenation-level-dependent (BOLD) (15,16), BF (17), and blood volume (18) changes in the retina associated with physiological gas challenges have been reported. Visual stimulations have also been studied using BOLD (19,20), blood volume (21), and manganese (22) contrast. MRI has been applied to study retinal degeneration (15,23), diabetic retinopathy (24), and glaucoma (25) in rodents. MRI also provides unique opportunities to study pharmacological responses to drugs (26-31).

In this study, we employed MRI to investigate the effects of nitroprusside on chorioretinal BF and oxygenation in rats. Graded nitroprusside was administered intravenously, and BF and BOLD MRI were simultaneously measured using the continuous arterial spin labeling (CASL) technique on an 11.7T scanner. Oxygen measurements were also made with a fiber optic oxygen probe to corroborate MRI findings. To our knowledge, this is the first use of MRI to study chorioretinal BF drug responses.

Materials and Methods

Animal preparation

All animal experiments were performed with IACUC approval and in accordance with the ARVO Statement for the Use of Animals in Ophthalmic and Vision Research. Adult male Long-Evans rats (total n = 13, 250–300 g; n = 10 for MRI studies and n = 3 for pO_2 measurement) were initially anesthetized with 2% isoflurane, intubated, and mechanically ventilated (Harvard small animal ventilator, Model 683, Harvard Apparatus, South Natick, MA). The respiratory rate of the ventilator was set between 57-60 bpm. The right femoral artery was then cannulated with PE-50 tubing for mean arterial blood pressure (MABP) and arterial blood gas measurement (Model ABL5, Radiometer Inc., Westlake, OH). MABP was continuously recorded via the arterial line to a BIOPAC system (Acknowledge, Santa Barbara, CA). The right femoral vein was also catheterized with PE-50 tubing for sodium nitroprusside infusion. A 23-gauge needle was inserted in the intraperitoneal space of the animal and extended via PE-50 tubing for pancuronium bromide administration (4 mg/kg/hr).

After the surgery, the isoflurane level was reduced to 1.2–1.5% and the animal was then placed on a custom-built head holder and secured with ear bars and tooth bar. An atropine eye drop was applied topically to dilate the pupil and reduce iris motion artifact (20). The body temperature was maintained at 37.0 ± 0.5 °C using a feedback-regulated circulating warm water pad. End-tidal CO_2 was continuously monitored (capnograph, Surgevet) and kept within normal physiological ranges. The heart rate and blood oxygen saturation level were recorded using a MouseOx system (STARR Life Science Corp., Oakmont, PA) and maintained within normal physiological ranges. Arterial pCO_2 and pO_2 were measured and kept between 35–40 mmHg and 90–110 mmHg, respectively, unless otherwise noted.

MRI measurements were made during intravenous nitroprusside (Sigma-Aldrich, St. Louis, MO) infusion of 1, 2, 3, 4 and 5 μg/kg/min in (n = 7, total 27 trials). The order of various doses was randomized. For ease of presentation, these were also separated into two groups: a low dose (1 and 2 μg/kg/min, iv) and a high dose (3, 4 and 5 μg/kg/min, iv). Vehicle control (same infusion volume of saline) was performed in a separate group of animals (n = 3, total 9 trials). A trial included 3 min baseline, 3 min during infusion, and again 3 min baseline. In the nitroprusside infusion group, 3-5 trials of each dose of nitroprusside were repeated in each animal with 10 min between trials to ensure that MABP had returned to

baseline, i.e., between 90–120 mmHg. Fiber-optic oxygen measurements were made under identical experimental conditions.

MRI acquisition

MRI studies were performed on an 11.7T/16cm magnet and a 74G/cm B-GA9S gradient insert (Bruker, Billerica, MA). A custom-made small circular surface coil (ID~7 mm) was placed on the left eye. Magnetic field homogeneity was optimized using FASTMAP shimming with first order shims on an isotropic voxel of 7×7×7 mm, encompassing the entire eye. Scout images were acquired to plan a single mid-sagittal slice bisecting the center of the eye and optic nerve for subsequent imaging in order to minimize partial-volume effect due to the retinal curvature (32,33). Combined BOLD and BF fMRI was acquired using the CASL technique (34) with single-shot, gradient echo planar imaging acquisition, spectral width = 192 kHz, TR = 3000 ms, TE = 13.3 ms, labeling duration = 2.9 s, FOV = 9×9 mm, slice thickness = 1 mm, acquisition matrix = 90×90, yielding an in-plane resolution = 100×100 μm and temporal resolution = 6 s. This spatial resolution did not distinguish retinal and choroidal BF, and thus the reported values are for combined chorioretinal BF.

Phantom studies confirmed nitroprusside which has a diamagnetic iron (Fe^{2+}) center exerted no T_2* contrast at very high (100 μg/ml) concentration as expected (data not shown).

pO_2 measurement

Vitreous pO_2 adjacent to the retina was measured by a fiber optic pO_2 probe with a ruthenium compound tip, whose fluorescence is quenched by oxygen (FOXY-AL300; Ocean Optics, Dunedin, FL). Note that this measurement primarily reflected retina tissue oxygenation and was different from arterial pO_2 (35). Calibration of the pO_2 probe was performed at 37° C in water equilibrated with 0%, 21%, 30%, and 100% O_2 using balanced N_2. The calibrated probe was inserted into the eye through a 21-gauge needle with a rubber valve to seal the space between the probe and the needle so as to prevent intraocular pressure change. The needle/probe was inserted via a micromanipulator through the sclera into the vitreous, and advanced until it touched the retina. The probe was then retracted about 500 μm (35). The location of the probe was confirmed as revealed by a sudden change in pO_2 reading by delivering 100% O_2 to animals via the ventilator, which increased vitreous pO_2.

Data analysis

Image analysis was performed using custom-written programs in Matlab (Math-Works, Natick, MA), STIMULATE (University of Minnesota), and Statistical Parametric Mapping (SPM) as described previously (33,36). Briefly, time series MRI data were co-registered using SPM and Matlab codes. The non-labeled images of the time-series CASL data were taken as BOLD data. Cross-correlation (CC) analysis of time-series data was performed using STIMULATE to obtain activation maps and the activated pixels were sampled to generate time-course data. Percent BOLD and BF changes in the retina were calculated and displayed by scatter plots. Statistical analyses of blood-gas and vitreous pO_2 data were performed by paired t-tests. MRI data in text were expressed in mean ± SD and compared by independent t-tests. $p < 0.05$ was used to indicate statistical significance.

Results

Table 1 summarizes the physiological parameters before and during the lowest (1μg/kg/min) and the highest (5 μg/kg/min) dose of nitroprusside infusion. Nitroprusside had no effect on arterial pO_2, pCO_2 and pH. Normal MABP was 107 ± 18 mmHg. Low dose nitroprusside decreased MABP by 18 ± 11 mmHg ($p < 0.01$ versus baseline), and high doses decreased

MABP by 42 ± 14 mmHg ($p < 0.01$ versus baseline). MABP's for the two nitroprusside doses were statistically different from each other ($p = 0.0006$).

Figure 1 shows the quantitative basal BF image, and the BF and BOLD responses to 2 μg/kg/min nitroprusside infusion. Basal BF values in the chorioretina and the ciliary body were high, whereas BF in the lens, cornea, and vitreous were within noise level as reported previously (32,37). Positive BF but negative BOLD responses were observed in the chorioretina following systemic nitroprusside infusion of 2 μg/kg/min, indicating a BF–BOLD uncoupling.

At 2 μg/kg/min dose, BF increased and BOLD signal decreased (Figure 2a), whereas at 4 μg/kg/min dose, BF showed sustained reduction during nitroprusside infusion and BOLD signal decreased (Figure 2b). Group data showed that the low dose (1-2 μg/kg/min, iv) nitroprusside infusion increased chorioretinal BF by 22.2 ± 14.6 % and decreased BOLD by 5.2 ± 0.6 %, whereas high dose (3-5 μg/kg/min, iv) nitroprusside infusion decreased chorioretinal BF and BOLD by 18.4 ± 10.9 % ($p = 0.00000002$, compared with low dose) and 7.7 ± 1.9 % ($p = 0.003$, compared with low dose), respectively. Vehicle infusion of the same volume showed no effect ($p > 0.05$) on BOLD and BF signals (Figure 2c). Figure 3 shows the BF and BOLD changes versus MABP ($n = 7$, total 27 trials). Both BF and BOLD were correlated with MABP decreases ($r = 0.75$, $p = 0.000007$, and $r = 0.52$, $p = 0.005$, respectively). Positive BF responses were observed with smaller MABP changes (i.e., < 30 mmHg), whereas negative BF responses were primarily observed with larger MABP changes (i.e., > 30 mmHg). BOLD responses were negative in all 27 trials.

Oxygen-electrode measurements showed that the vitreous pO_2 at the vitreoretinal boundary decreased by −6.4 ± 2.9% and −19.9 ± 5.8% at low and high dose, respectively (Figure 4). The vitreous pO_2 changes were significantly different between the two doses ($p = 0.009$).

Discussion

This study investigated BF MRI and BOLD MRI responses to graded nitroprusside infusions in the rat retina. The major findings are: (i) nitroprusside has no effect on arterial pO_2, pCO_2, and pH but decreased MABP in a dose dependent manner, (ii) nitroprusside at low dose (1 and 2 μg/kg/min) evoked positive BF and negative BOLD responses with mild MABP reduction, (iii) nitroprusside at higher dose (3, 4 and 5 μg/kg/min) evoked negative BF and larger negative BOLD responses with large MABP reduction, (iv) nitroprusside decreases vitreous pO_2 (at the vitreoretinal boundary) as measured by oxygen electrode in a dose dependent manner. To our knowledge, this is the first pharmacological MRI application in the retina. These results showed an apparent BF and BOLD uncoupling *in vivo* and these findings could have important implications of tissue hypoxia for patients treated with nitroprusside.

The advantages of BF MRI are that it can measure tissue perfusion in classical quantitative units non-invasively with a large field of view that it is not depth limited (32). The disadvantages are it takes significantly longer to acquire and it is not as cost effective compared to optical techniques. BF MRI may have the unique potential to image quantitative retinal and choroidal specific BF without depth ambiguity *in vivo* if higher spatial resolution can be achieved. Note that choroidal BF is about 7 times higher than retinal BF as measured by CASL MRI in mice (37) and 11 times higher than retinal BF as measured by microsphere technique in rats (38). In the present study, the BF and BOLD MRI changes were likely dominated by the choroid based on BF alone. It is possible that the retinal and choroidal vessels may be affected differently by nitroprusside and its effect on MABP. MRI may also have potential to depict optic nerve hemodynamic responses as

shown in Figure 1. However, this was not consistently observed across subjects as the RF coil was not optimized for optical nerve imaging.

At high dose, nitroprusside decreased MABP by 42 ± 14 mmHg and chorioretinal BF by 18 %. Blood flow showed strong decreases without recovery to the baseline up to 6 mins after the onset of infusion. This is likely due to strong systemic vasodilation, resulting in large MABP drop. Such MABP drop not only affected the retina but also affected the entire body which could cause “blood-steal” effect away from the retina because other organs have large mass substantially drawing more blood and taking longer time to recover (39-41). The proportionally greater drop in MABP than BF indicates chorioretinal vasodilation. Our findings are consistent with a rat study which showed that choroidal BF decreased linearly with MABP when MABP dropped by more than 40 mmHg (42). The drop in BF presumably led to the decreased chorioretinal BOLD signal, since the arterial pO_2 and pCO_2 were unchanged. This finding is consistent with a nitroglycerin (another NO donor) study in which oxygen saturation of the retinal venous blood fell 13% in response to nitroglycerin, despite vasodilation of both retinal arteries and veins (43).

At low dose, nitroprusside increased chorioretinal BF by 22 % despite a mild drop in MABP (18 ± 11 mmHg), in agreement with the 10–30% increases elicited in human retinal BF by nitroprusside (0.5–2 μg/kg/min) obtained with the blue field entoptic technique (12). Nitroprusside has been reported to increase retinal arteriolar and venular diameter in rats (9,10) and humans (12), and to dilate retinal and choroid vessels in newborn pigs (11). In the present study, BF increase at low dose likely occurred because the decrease in vascular resistance was proportionally greater than the mild MABP drop. BF showed recovery toward the baseline prior to the end of infusion at both low and high nitroprusside doses. This may be associated with autoregulation of the retinal circulation (44-46) and choroid (47), which tends to counter the initial acute hypo- or hypertension.

Surprisingly, BOLD signals decreased despite the chorioretinal BF increase during low dose nitroprusside. Such BOLD-BF uncoupling is rarely reported in the brain imaging literature. A brain fMRI study reported widespread negative BOLD responses in multiple brain regions after nitroprusside injection with only a few areas (i.e., ventral hypothalamus and amygdala) showing positive BOLD responses (48). BF was not measured in that study. A likely explanation is that nitroprusside dilates venous vessels. An increase in venous blood volume likely decreases BOLD signal in the choroid in the absence of arterial pO_2 changes, which could explain the BOLD-BF uncoupling. There is evidence in the treatment of acute decompensated heart failure that nitroprusside rapidly increased venous capacity and reduced arterial resistance (2,3). Another alternative explanation is that nitroprusside increased oxygen consumption in the retina. However, a positron emission tomography study of the brain revealed no changes in oxygen consumption associated with nitroprusside infusion (16 μg/kg/min) (49), although MABP-BF regulation of the brain might be different from that of the retina and choroid.

Fiber-optic oxygen measurements corroborated the BOLD fMRI findings. Nitroprusside decreased vitreous pO_2 by 6-20% in a dose-dependent manner, consistent with similar oxygen electrode measurements in rat (50) and dog (51) brains which reported that nitroprusside produced hypotension and decreased brain tissue pO_2. A possible explanation for decreased vitreous pO_2 associated with nitroprusside could be due to the arteriovenous shunting effect of nitroprusside (51). Endrich et al., showed nitroprusside dilated arterioles and decreased precapillary resistance, but has less effect on changing venular diameter, causing the arteriovenous pressure gradient to be reduced by more than 50% and decreased functional capillary density, thus tissue hypoxia. In contrast, nitroglycerin dilated both arterioles and venules whereas no tissue hypoxia was observed (52). Ogawa et al. also found

nitroprusside had a stronger vasodilatory effect on retinal arteries than veins (9,10), implying the arteriovenous pressure gradient could also shift downward in the retina and induce retinal tissue hypoxia.

Retinal and choroidal BOLD responses to hypoxic challenge have been recently reported in mice using balanced steady-state free-precession (bSSFP) MRI (53). The signal dropped 26% in the choroid and 11% in the retina when breathing 10% oxygen, indicating MR BOLD sensitivity to blood oxygen saturation in the retina/choroid. BF was not measured in that study. The graded nitroprusside responses showed some similarities to those of the mild and severe hypoxia responses reported in the brain (54). As inhaled oxygen tension decreases below ~10%, cerebral BF increases and vessel dilate substantially to compensate. BF increase is insufficient to bring tissue oxygen tension to the same level as normoxia, and thus BOLD signal decreases. There could also be an increase in venous blood volume, which would further reduce the BOLD signal, in addition to the oxygen tension change. As inhaled oxygen tension is decreased further (<7%, dependent on other experimental conditions), vessels become maximally dilated and MABP falls, such that cerebral BF and BOLD signals decrease precipitously.

Conclusion

This study demonstrates a novel MRI application to study pharmacological effects in the retina. This non-invasive MRI approach offers opportunities to investigate ocular hemodynamics and evaluate the effects of novel therapeutic interventions on oxygenation and BF in the normal and diseased retinas. Future studies will improve spatial resolution to visualize potential differential responses in the retinal and choroid circulation as they could be regulated differently (47,55,56), and could have different susceptibility to MABP changes (57-59).

Acknowledgments

Grant support: This work was supported in part by the NIH/NEI (R01 EY009702, EY014211 and EY018855), MERIT Award from the Department of Veterans Affairs, and San Antonio Life Science Institute to TQD and American Heart Association (10POST4290091), Clinical Translational Science Award (CTSA, parent grant UL1RR025767), and San Antonio Area Foundation to YYIS.

References

1. Palmer RM, Ferrige AG, Moncada S. Nitric oxide release accounts for the biological activity of endothelium-derived relaxing factor. Nature. 1987; 327(6122):524–526. [PubMed: 3495737]
2. Opasich C, Cioffi G, Gualco A. Nitroprusside in decompensated heart failure: what should a clinician really know? Curr Heart Fail Rep. 2009; 6(3):182–190. [PubMed: 19723460]
3. Mullens W, Abrahams Z, Francis GS, Skouri HN, Starling RC, Young JB, Taylor DO, Tang WH. Sodium nitroprusside for advanced low-output heart failure. J Am Coll Cardiol. 2008; 52(3):200–207. [PubMed: 18617068]
4. Tinker JH, Michenfelder JD. Sodium nitroprusside: pharmacology, toxicology and therapeutics. Anesthesiology. 1976; 45(3):340–354. [PubMed: 962181]
5. Schmetterer L, Wolzt M, Salomon A, Rheinberger A, Unfried C, Zanaschka G, Fercher AF. Effect of isoproterenol, phenylephrine, and sodium nitroprusside on fundus pulsations in healthy volunteers. Br J Ophthalmol. 1996; 80(3):217–223. [PubMed: 8703859]
6. Schmetterer L, Polak K. Role of nitric oxide in the control of ocular blood flow. Prog Retin Eye Res. 2001; 20(6):823–847. [PubMed: 11587919]
7. Mann RM, Riva CE, Stone RA, Barnes GE, Cranstoun SD. Nitric oxide and choroidal blood flow regulation. Invest Ophthalmol Vis Sci. 1995; 36(5):925–930. [PubMed: 7706041]

8. Huemer KH, Garhofer G, Aggermann T, Kolodjaschna J, Schmetterer L, Fuchsjager-Mayrl G. Role of nitric oxide in choroidal blood flow regulation during light/dark transitions. Invest Ophthalmol Vis Sci. 2007; 48(9):4215–4219. [PubMed: 17724209]
9. Ogawa N, Saito M, Mori A, Sakamoto K, Kametaka S, Nakahara T, Ishii K. Vasodilator effect of nicorandil on retinal blood vessels in rats. Naunyn Schmiedebergs Arch Pharmacol. 2007; 375(5): 323–328. [PubMed: 17525845]
10. Ogawa N, Mori A, Hasebe M, Hoshino M, Saito M, Sakamoto K, Nakahara T, Ishii K. Nitric oxide dilates rat retinal blood vessels by cyclooxygenase-dependent mechanisms. Am J Physiol Regul Integr Comp Physiol. 2009; 297(4):R968–977. [PubMed: 19625688]
11. Hardy P, Nuyt AM, Abran D, St-Louis J, Varma DR, Chemtob S. Nitric oxide in retinal and choroidal blood flow autoregulation in newborn pigs: interactions with prostaglandins. Pediatr Res. 1996; 39(3):487–493. [PubMed: 8929870]
12. Polak K, Dorner G, Kiss B, Polska E, Findl O, Rainer G, Eichler HG, Schmetterer L. Evaluation of the Zeiss retinal vessel analyser. Br J Ophthalmol. 2000; 84(11):1285–1290. [PubMed: 11049956]
13. Berkowitz BA, Luan H, Gupta RR, Pacheco D, Seidner A, Roberts R, Liggett J, Knoerzer DL, Connor JR, Du Y, Kern TS, Ito Y. Regulation of the early subnormal retinal oxygenation response in experimental diabetes by inducible nitric oxide synthase. Diabetes. 2004; 53(1):173–178. [PubMed: 14693712]
14. Donati G, Pournaras CJ, Tsacopoulos M. Effect of nitroprusside on arteriolar constriction after retinal branch vein occlusion. Invest Ophthalmol Vis Sci. 1998; 39(10):1910–1917. [PubMed: 9727414]
15. Cheng H, Nair G, Walker TA, Kim MK, Pardue MT, Thule PM, Olson DE, Duong TQ. Structural and functional MRI reveals multiple retinal layers. Proc Natl Acad Sci USA. 2006; 103:17525–17530. [PubMed: 17088544]
16. Zhang Y, Peng Q, Kiel JW, Rosende CA, Duong TQ. Magnetic resonance imaging of vascular oxygenation changes during hyperoxia and carbogen challenges in the human retina. Invest Ophthalmol Vis Sci. 2011; 52(1):286–291. [PubMed: 20847121]
17. Peng Q, Zhang Y, Nateras OS, van Osch MJ, Duong TQ. MRI of blood flow of the human retina. Magn Reson Med. 2011; 65(6):1768–1775. [PubMed: 21590806]
18. Nair G, Shen Q, Duong TQ. Relaxation Time Constants and Apparent Diffusion Coefficients of Rat Retina at 7 Tesla. International Journal of Imaging Systems and Technology. 2010; 20:126–130.
19. Duong TQ, Ngan SC, Ugurbil K, Kim SG. Functional Magnetic Resonance Imaging of the Retina. Invest Ophthalmol Vis Sci. 2002; 43:1176–1181. [PubMed: 11923263]
20. De La Garza BH, Muir ER, Li G, Shih YY, Duong TQ. Blood oxygenation level-dependent (BOLD) functional MRI of visual stimulation in the rat retina at 11.7 T. NMR in biomedicine. 2011; 24(2):188–193. [PubMed: 21344533]
21. Shih YY, De la Garza BH, Muir ER, Rogers WE, Harrison JM, Kiel JW, Duong TQ. Lamina-specific functional MRI of retinal and choroidal responses to visual stimuli. Invest Ophthalmol Vis Sci. 2011; 52(8):5303–5310. [PubMed: 21447679]
22. Berkowitz BA, Roberts R, Goebel DJ, Luan H. Noninvasive and simultaneous imaging of layer-specific retinal functional adaptation by manganese-enhanced MRI. Invest Ophthalmol Vis Sci. 2006; 47(6):2668–2674. [PubMed: 16723485]
23. Li Y, Cheng H, Shen Q, Kim M, Thule PM, Olson DE, Pardue MT, Duong TQ. Blood-Flow Magnetic Resonance Imaging of Retinal Degeneration. Invest Ophthalmol Vis Sci. 2009; 50:1824–1830. [PubMed: 18952917]
24. Berkowitz BA, Roberts R, Luan H, Peysakhov J, Mao X, Thomas KA. Dynamic contrast-enhanced MRI measurements of passive permeability through blood retinal barrier in diabetic rats. Invest Ophthalmol Vis Sci. 2004; 45(7):2391–2398. [PubMed: 15223822]
25. Calkins DJ, Horner PJ, Roberts R, Gradianu M, Berkowitz BA. Manganese-enhanced MRI of the DBA/2J mouse model of hereditary glaucoma. Invest Ophthalmol Vis Sci. 2008; 49(11):5083–5088. [PubMed: 18552381]
26. Leslie RA, James MF. Pharmacological magnetic resonance imaging: a new application for functional MRI. Trends Pharmacol Sci. 2000; 21(8):314–318. [PubMed: 10918638]

27. Chen YC, Mandeville JB, Nguyen TV, Talele A, Cavagna F, Jenkins BG. Improved mapping of pharmacologically induced neuronal activation using the IRON technique with superparamagnetic blood pool agents. J Magn Reson Imaging. 2001; 14(5):517–524. [PubMed: 11747003]
28. Chen YC, Galpern WR, Brownell AL, Matthews RT, Bogdanov M, Isacson O, Keltner JR, Beal MF, Rosen BR, Jenkins BG. Detection of dopaminergic neurotransmitter activity using pharmacologic MRI: correlation with PET, microdialysis, and behavioral data. Magn Reson Med. 1997; 38(3):389–398. [PubMed: 9339439]
29. Jenkins BG, Sanchez-Pernaute R, Brownell AL, Chen YC, Isacson O. Mapping dopamine function in primates using pharmacologic magnetic resonance imaging. J Neurosci. 2004; 24(43):9553–9560. [PubMed: 15509742]
30. Gozzi A, Ceolin L, Schwarz A, Reese T, Bertani S, Crestan V, Bifone A. A multimodality investigation of cerebral hemodynamics and autoregulation in pharmacological MRI. Magnetic resonance imaging. 2007; 25(6):826–833. [PubMed: 17451905]
31. Schwarz AJ, Gozzi A, Reese T, Bifone A. In vivo mapping of functional connectivity in neurotransmitter systems using pharmacological MRI. NeuroImage. 2007; 34(4):1627–1636. [PubMed: 17188903]
32. Li Y, Cheng H, Duong TQ. Blood-flow magnetic resonance imaging of the retina. NeuroImage. 2008; 39(4):1744–1751. [PubMed: 18063388]
33. Cheng H, Nair G, Walker TA, Kim MK, Pardue MT, Thule PM, Olson DE, Duong TQ. Structural and functional MRI reveals multiple retinal layers. Proceedings of the National Academy of Sciences of the United States of America. 2006; 103(46):17525–17530. [PubMed: 17088544]
34. Shen Q, Meng X, Fisher M, Sotak CH, Duong TQ. Pixel-by-pixel spatiotemporal progression of focal ischemia derived using quantitative perfusion and diffusion imaging. J Cereb Blood Flow Metab. 2003; 23(12):1479–1488. [PubMed: 14663344]
35. Yu DY, Cringle SJ, Alder VA. The response of rat vitreal oxygen tension to stepwise increases in inspired percentage oxygen. Invest Ophthalmol Vis Sci. 1990; 31(12):2493–2499. [PubMed: 2265989]
36. Duong TQ, Pardue MT, Thule PM, Olson DE, Cheng H, Nair G, Li Y, Kim M, Zhang X, Shen Q. Layer-specific anatomical, physiological and functional MRI of the retina. NMR in biomedicine. 2008; 21(9):978–996. [PubMed: 18792422]
37. Muir ER, Duong TQ. MRI of retinal and choroidal blood flow with laminar resolution. NMR in biomedicine. 2011; 24(2):216–223. [PubMed: 20821409]
38. Wang L, Grant C, Fortune B, Cioffi GA. Retinal and choroidal vasoreactivity to altered PaCO2 in rat measured with a modified microsphere technique. Exp Eye Res. 2008; 86(6):908–913. [PubMed: 18420196]
39. Harel N, Lee SP, Nagaoka T, Kim DS, Kim SG. Origin of negative blood oxygenation level-dependent fMRI signals. J Cereb Blood Flow Metab. 2002; 22(8):908–917. [PubMed: 12172376]
40. Shmuel A, Yacoub E, Pfeuffer J, Van de Moortele PF, Adriany G, Hu X, Ugurbil K. Sustained negative BOLD, blood flow and oxygen consumption response and its coupling to the positive response in the human brain. Neuron. 2002; 36(6):1195–1210. [PubMed: 12495632]
41. Koss MC. Functional role of nitric oxide in regulation of ocular blood flow. Eur J Pharmacol. 1999; 374(2):161–174. [PubMed: 10422757]
42. Reiner A, Li C, Del Mar N, Fitzgerald ME. Choroidal blood flow compensation in rats for arterial blood pressure decreases is neuronal nitric oxide-dependent but compensation for arterial blood pressure increases is not. Exp Eye Res. 2010; 90(6):734–741. [PubMed: 20302861]
43. Frayser R, Hickam JB. Effect of Vasodilator Drugs on the Retinal Blood Flow in Man. Arch Ophthalmol. 1965; 73:640–642. [PubMed: 14281979]
44. Riva CE, Grunwald JE, Petrig BL. Autoregulation of Human Retinal Blood-Flow - an Investigation with Laser Doppler Velocimetry. Invest Ophthalmol Vis Sci. 1986; 27(12):1706–1712. [PubMed: 2947873]
45. Ffytche TJ, Bulpitt CJ, Kohner EM, Archer D, Dollery CT. Effect of changes in intraocular pressure on the retinal microcirculation. Br J Ophthalmol. 1974; 58(5):514–522. [PubMed: 4418478]
46. Kaufman, PL.; Alm, A., editors. Adler's Physiology of the Eye. St Louis: Mosby; 1992.

47. Kiel JW. Choroidal myogenic autoregulation and intraocular pressure. Exp Eye Res. 1994; 58(5): 529–543. [PubMed: 7925690]
48. Henderson LA, Richard CA, Macey PM, Runquist ML, Yu PL, Galons JP, Harper RM. Functional magnetic resonance signal changes in neural structures to baroreceptor reflex activation. J Appl Physiol. 2004; 96(2):693–703. [PubMed: 14565965]
49. Schumann-Bard P, Touzani O, Young AR, Toutain J, Baron JC, Mackenzie ET, Schmidt EA. Cerebrovascular effects of sodium nitroprusside in the anaesthetized baboon: a positron emission tomographic study. J Cereb Blood Flow Metab. 2005; 25(4):535–544. [PubMed: 15703704]
50. Seyde WC, Longnecker DE. Cerebral oxygen tension in rats during deliberate hypotension with sodium nitroprusside, 2-chloroadenosine, or deep isoflurane anesthesia. Anesthesiology. 1986; 64(4):480–485. [PubMed: 3963454]
51. Hoffman WE, Edelman G, Ripper R, Koenig HM. Sodium nitroprusside compared with isoflurane-induced hypotension: the effects on brain oxygenation and arteriovenous shunting. Anesth Analg. 2001; 93(1):166–170. [PubMed: 11429359]
52. Endrich B, Franke N, Peter K, Messmer K. Induced hypotension: action of sodium nitroprusside and nitroglycerin on the microcirculation. A micropuncture investigation. Anesthesiology. 1987; 66(5):605–613. [PubMed: 3107434]
53. Muir ER, Duong TQ. Layer-specific functional and anatomical MRI of the retina with passband balanced SSFP. Magn Reson Med. 2011
54. Duong TQ, Iadecola C, Kim SG. Effect of hyperoxia, hypercapnia, and hypoxia on cerebral interstitial oxygen tension and cerebral blood flow. Magn Reson Med. 2001; 45(1):61–70. [PubMed: 11146487]
55. Kiel JW, Shepherd AP. Autoregulation of choroidal blood flow in the rabbit. Invest Ophthalmol Vis Sci. 1992; 33(8):2399–2410. [PubMed: 1634337]
56. Kiel JW. Modulation of choroidal autoregulation in the rabbit. Exp Eye Res. 1999; 69(4):413–429. [PubMed: 10504275]
57. Bill A, Sperber GO. Control of retinal and choroidal blood flow. Eye (Lond) . 1990; 4(Pt 2):319–325. [PubMed: 2199239]
58. Polak K, Polska E, Luksch A, Dorner G, Fuchsjager-Mayrl G, Findl O, Eichler HG, Wolzt M, Schmetterer L. Choroidal blood flow and arterial blood pressure. Eye (Lond) . 2003; 17(1):84–88. [PubMed: 12579176]
59. Friedman E. Choroidal blood flow. Pressure-flow relationships. Arch Ophthalmol. 1970; 83(1):95–99. [PubMed: 5411694]

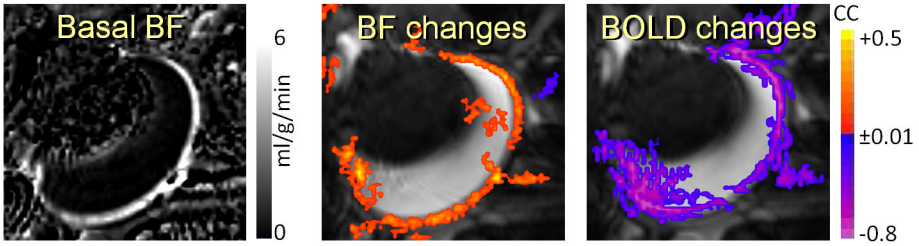

Figure 1.
Basal BF and nitroprusside-induced BF and BOLD changes in the retina/choroid from a representative subject (2 μg/kg/min, i.v.). Nitroprusside infusion increased BF but decreased BOLD signal in the retina/choroid.

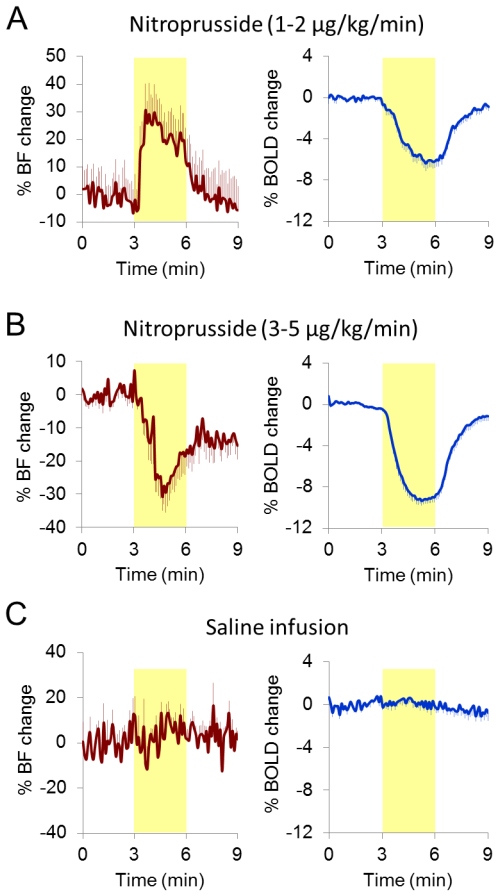

Figure 2.

Averaged pharmacological MRI time-courses. Yellow-shaded regions indicate the nitroprusside infusion durations. **(a)** Nitroprusside infusion increased BF but decreased BOLD signal in the retina/choroid at low dose (13 trials). **(b)** At high dose, BF showed sustained reduction and BOLD signal decreased (14 trials). **(c)** Saline infusion showed no effect on BF and BOLD signals (9 trials).

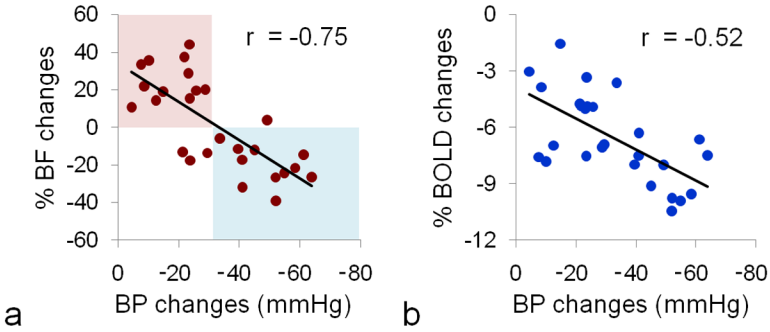

Figure 3.

Nitroprusside-induced arterial BP, chorioretinal BF and BOLD changes (n = 7, total 27 trials). Significant linear correlation was observed between BF and MABP changes (p=0.000007) and between BOLD and MABP changes (p=0.005). Positive BF responses were mainly observed with smaller MABP changes (i.e., lower nitroprusside dosage, red-shaded area), whereas negative BF responses were mainly observed with larger MABP changes (i.e., higher nitroprusside dosage, blue-shaded area). No positive BOLD response was observed across 27 trials.

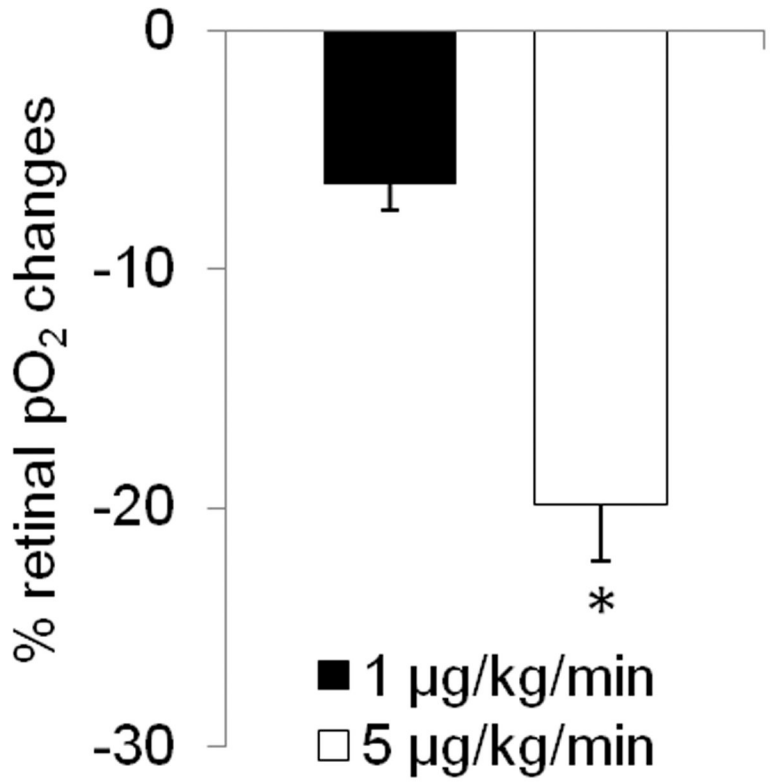

Figure 4.

Effect of nitroprusside infusion on vitreous pO_2 (at the vitreoretinal boundary) changes as measured by fiber optic oxygen probe (n = 3). Both the lowest and the highest infusion doses showed vitreous pO_2 reduction. The vitreous pO_2 changes were significantly stronger with 5 μg/kg/min than 1 μg/kg/min nitroprusside infusion (p=0.009). Error bars are s.e.m. values.

Table 1

Arterial pO_2 and pCO_2 (in mmHg) before and during nitroprusside infusion (n = 4, total 7 trials).

	1 μg/kg/min		5 μg/kg/min	
	baseline	**nitroprusside**	**baseline**	**nitroprusside**
Arterial pO_2	100 ± 7	102 ± 7	102 ± 5	103 ± 8
Arterial pCO_2	32 ± 2	31 ± 2	31 ± 2	30 ± 4